Published in final edited form as:
Bone. 2006 October ; 39(4): 767–772. doi:10.1016/j.bone.2006.04.006.

Alteration of femoral bone morphology and density in COX-2−/− mice

Galen Robertson[a], **Chao Xie**[b], **Di Chen**[b], **Hani Awad**[b], **Edward M. Schwarz**[b], **Regis J. O'Keefe**[b], **Robert E. Guldberg**[a], and **Xinping Zhang**[b,*]

a *Parker H. Petit Institute for Bioengineering and Bioscience, Georgia Institute of Technology, Atlanta, GA 30332, USA*

b *Center for Musculoskeletal Research, University of Rochester Medical Center, 601 Elmwood Avenue, Rochester, NY 14642, USA*

Abstract

A role of COX-2 in pathological bone destruction and fracture repair has been established; however, few studies have been conducted to examine the involvement of COX-2 in maintaining bone mineral density and bone micro-architecture. In this study, we examined bone morphology in multiple trabecular and cortical regions within the distal and diaphyseal femur of 4-month-old wild-type and COX-2−/− mice using micro-computed tomography. Our results demonstrated that while COX-2−/− female mice had normal bone geometry and trabecular microarchitecture at 4 months of age, the male knockout mice displayed reduced bone volume fraction within the distal femoral metaphysis. Furthermore, male COX-2−/− mice had a significant reduction in cortical bone mineral density within the central cortical diaphysis and distal epiphysis and metaphysis. Consistent with the observed reduction in cortical mineral density, biomechanical testing via 4-point-bending showed that male COX-2−/− mice had a significant increase in postyield deformation, indicating a ductile bone phenotype in male COX-2−/− mice. In conclusion, our study suggests that genetic ablation of COX-2 may have a sex-related effect on cortical bone homeostasis and COX-2 plays a role in maintaining normal bone micro-architecture and density in mice.

Keywords

COX-2; Bone mineral density (BMD); Postyield deflection (YPD)

Introduction

Prostaglandin G/H synthase, also known as cyclooxygenase, catalyzes the conversion of arachidonic acid to prostaglandins. At least two isoforms of cyclooxygenase have been identified, COX-1 and COX-2 [20,26,34]. COX-1 is a constitutive enzyme present in most mammalian cells. In contrast, measurable COX-2 gene expression normally occurs in only a few cell types, but its expression can be induced in many if not all cells by a variety of external stimuli [9]. Among those that are related to bone metabolism are mechanical loading [6,38], BMP-2 [5], PTH [36], FGF2, TGF-β [17,29] and a variety of inflammatory cytokines such as IL-1, IL-6 and TNF-α [39]. Based on the unique expression pattern of the two isoforms, it is thought that COX-2 is the immediate early gene involved in modulating inflammation, carcinogenesis, and cell mitosis and differentiation. In contrast, COX-1 functions as a housekeeping gene for maintaining the homeostasis of cells. Genetic ablation of COX-1 or

*Corresponding author. Fax: +1 716 275 1121. E-mail address: Xinping_Zhang@URMC.rochester.edu (X. Zhang).

COX-2 in mice demonstrates the distinctive yet overlapping functions of these two enzymes in a variety of physiological and pathological processes. In comparison to COX-1−/− mice, which survive well and appear generally healthy, COX-2−/− mice have a limited life span due to severe nephropathy, cardiac fibrosis and increased susceptibility of peritonitis [22,24].

Prostaglandins that are generated through COX activities act locally as important micro-environmental hormones mediating autocrine and/or paracrine functions. Prostaglandins have shown both anabolic and catabolic effects on bone metabolism [12,30,31,40]. Recent studies using COX-1−/− and COX-2−/− mice demonstrate that COX-2 is involved in high bone turnover such as inflammation-mediated bone osteolysis in vivo. Genetic ablation of COX-2 results in reduced osteoclastogenesis in bone marrow culture and minimized bone destruction in animal models of prosthetic implant loosening [27,42]. COX-2 is also involved in osteoblastic bone formation in response to growth factors and anabolic growth factors such as FGF-1 [43]. In addition, COX-2 is shown to be essential for bone fracture healing [33,43] and inhibition of COX-2 has been shown to impair bone ingrowth in animal models [8].

Besides hormone and growth factor regulations, mechanical stimulation is essential for maintaining bone mass and bone homeostasis. COX-2 is induced in an immediate early fashion in osteocytes by stretching, indicating an important role in mechanotransduction [13,18,23]. Fluid shear stress also induces COX-2 in MC3T3-E1 cells and the induction is mediated by both PKC and PKA pathways [37,38]. There is also evidence to show that COX-2 is involved in lamellar bone formation elicited by mechanical strain [6,7]. Treatment with NS398, a selective COX-2 inhibitor, abolishes the induction of endocortical but not periosteal bone formation by mechanical loading in vivo [7]. In view of the dual effects of COX-2 on both bone resorption and bone formation, the net effects of COX-2 gene on maintaining bone mass and modulating normal bone remodeling remain to be elucidated.

To further examine the role of COX-2 in maintaining bone mass, we performed microcomputed tomography (micro-CT) image analyses combined with biomechanical testing to determine the trabecular and cortical bone morphology, bone mineral density and mechanical properties of femurs obtained from COX-2−/− mice and their wild-type counterparts. Due to the poor survival rate of COX-2−/− mice beyond 4 months, we focused our analyses on paired littermates at 4 months of age. Our data demonstrate that genetic ablation of COX-2 led to a femoral bone phenotype that is characterized by significantly reduced metaphyseal bone volume fraction and significantly reduced cortical bone mineral density accompanied with altered biomechanical properties in male mice.

Materials and methods

Experimental animals

COX-2−/− mice were originally obtained from the breeding colony maintained at the University of North Carolina. They were further bred to 129/ola genetic background and intercrossed for about 30 generations. A total of 42 4-month-old mice were analyzed using micro-CT and biomechanical testing, which included 14 wild-type males and 13 COX-2−/− males, 7 wild-type females and 7 COX-2−/− females.

Microcomputed tomography

Indices of cortical and trabecular bone morphology from the distal and diaphyseal femur were assessed by micro-CT imaging (μCT 40, Scanco Medical, SUI). For all scans, a global threshold was applied to separate mineralized and soft tissues and kept consistent within each analysis region. Three separate regions were scanned at 16 μm voxel size for morphological and mineral density analyses (Fig. 1, shaded areas). Two regions were isolated within the distal femur, on

the distal and proximal side of the growth plate, consisting of epiphyseal and metaphyseal trabecular bone, respectively. The epiphyseal region began where the two condyles meet in the center of the femur and extended 0.32 mm towards the growth plate. The metaphyseal region began 0.05 mm proximal to the growth plate and extended 0.80 mm towards the diaphysis of the femur. In both trabecular regions, all cortical bone was excluded from the analyses by manual segmentation. For cortical bone analyses, a 1.0 mm section of cortical bone in the center of the diaphysis was scanned and evaluated. The area corresponded to the area tested in four-point bending (Fig. 1).

Analysis of bone morphology and microarchitecture

For morphometric analyses of trabecular bone, a direct 3D model [10,11] was used to determine the trabecular spacing (Tb.Sp), trabecular thickness (Tb. Th.), trabecular number (Tb.N.), trabecular connectivity (Conn.) and bone volume fraction (BVF). For cortical bone analyses, the cortical bone volume (Cort. BV) and cortical thickness (Cort. Th.) were measured by micro-CT. Three cross-sectional images were captured at 0.5 mm increments along the scanned cortical bone region. IMAQ Vision Builder (Labview) was used to calculate area, height, width of each cross-section and the moment of inertia at medial–lateral axis and anterior posterior axis (I_{ML} and I_{AP}). The length of femurs was measured by high precision calipers (Mitutoyo Inc., Japan). Each femur was measured three times and mean lengths were recorded.

Analysis of bone mineral density

Bone mineral density was measured by micro-CT in three scanned regions. The μCT 40 system was calibrated by scanning a series of four hydroxyapatite (HA) phantoms of known densities. A standard linear attenuation curve was then used to convert the data into a true mineral density value (mg HA/cm^3). Epiphyseal, metaphyseal and cortical bone regions were thresholded to obtain a binary image that closely matched the reconstructed grayscale image from the scans. Within each region, the threshold was kept constant for analyses of bones in all the mice.

Mechanical testing via four-point bending

The femora were tested to failure via four-point bending at a rate of 0.05 mm/s with a MTS 858 mechanical testing system. The distance between the lower supports spanned 6.2 mm, while the upper supports were separated by 2.2 mm. The support points had a radius of 0.5 mm. The upper supports were centered on the mid-diaphysis at the same location that was scanned by micro-CT. Each femur was tested in the anterior–posterior plane with the anterior side in tension and the posterior side in compression. Force and deflection data were directly measured with the MTS system. From these data, stiffness, yield force, maximum force, postyield deflection (PYD) and work to failure (Work) were calculated. Yield was defined as a 10% reduction in secant slope of the stiffness. Postyield deformation was defined as the amount of deformation from the point of yield to failure. Using the moment of inertia data collected from the micro-CT images, the force-deflection data were normalized to determine stress at failure and elastic modulus (E). The equation used to calculate stress was

$$\sigma = F\left(\frac{ac}{2I_{ML}}\right) \quad (1)$$

and for elastic modulus,

$$E=S\left(\frac{a^2}{12I_{\mathrm{ML}}}\right)(3L-4a) \quad (2)$$

where, σ = stress, F = applied force, c = 1/2 of anterior–posterior axis, a = horizontal distance between upper and lower supports (2 mm), I_{ML} = 2nd moment of area about the medial–lateral axis, E = Young's modulus, S = stiffness, L = horizontal distance between upper and lower supports (6.2 mm).

Statistical analysis

Analysis of variance (ANOVA) tests were performed to determine statistical significance. A general linear model with a univariate analysis of variance was used. Multiple comparison tests between groups were conducted using Minitab (Minitab Inc, State College, PA, USA). Data are presented as means ± SE. A P value <0.05 was considered statistically significant. A P value <0.10 was considered as a trend.

Results

Trabecular and cortical bone morphology

As expected, the effects of sex on bone morphology and micro-architecture were significant. In all regions examined, male mice exhibited higher morphometric indices than female littermates. The gross femur dimensions, including height, width and length of the femur were unchanged in COX-2−/− mice compared to their age and sex matched littermate controls. No differences as a function of genotype were observed in cortical bone cross-sectional geometry (Table 1). Trabecular bone micro-architecture was examined separately within the distal femoral metaphysis and epiphysis in wild-type and COX-2−/− mice (Table 2). COX-2−/− female mice exhibited similar microarchitecture compared to wild-type control mice in both regions, whereas COX-2−/− male mice demonstrated about 16% reduction of bone volume fraction (BVF) within the distal metaphyseal region of the male knockout mice (P <0.05). Albeit not statistically significant, male COX-2−/− mice also demonstrated reduced metaphyseal thickness and connectivity as well as increased trabecular separation at metaphyseal region. No significant differences were observed in epiphyseal trabecular bone micro-architecture in terms of bone volume fraction (BVF), trabecular spacing (Tb.Sp), trabecular thickness (Tb.Th.) and trabecular numbers (Tb.N.), yet knockout male COX-2−/−mice displayed increased trabecular connectivity compared to wild-type controls (P < 0.05).

Bone mineral density

Bone mineral density in cortical, epiphyseal and metaphyseal regions of femoral bone was measured using Micro-CT. All female mice, regardless of the genotypes, exhibited significantly higher bone mineral density than their age and genotype matched male counterparts at all three regions (P < 0.001) (Fig. 2). When compared with wild-type male mice, male COX-2−/− mice showed about 3% reduction in bone mineral density in the diaphyseal cortical region, metaphyseal and epiphyseal trabecular region. The differences were shown to be statistically significant (P < 0.001). Female COX-2−/− mice had an insignificant trend of decreased metaphyseal bone mineral density (P < 0.10), but at both epiphysis and cortical regions, bone mineral density was not significantly different from wild-type controls (P > 0.10).

Mechanical properties

Mechanical properties of the femurs from 4-month-old wild-type and COX-2−/− mice were examined using four-point bending. Differences in maximum force, yield force, ultimate stress, yield stress, work to failure and elastic modulus were observed between male and female mice, correlating with the differences observed in mid-diaphyseal morphology and mineral density (Table 3). When analyzed separately, COX-2−/−-male and female mice demonstrated similar mechanical properties compared to their wild-type controls in terms of stiffness, yield force and maximum force. However, postyield deflection (PYD), which should be highly sensitive to variations in mineral density, was found to be significantly increased by about 1.5-fold in male COX-2−/− mice at 4-month age ($P < 0.05$). The increased PYD was associated with a trend towards increased Work ($P < 0.10$) and decreased elastic modulus, indicating a more ductile bone in the male COX-2−/− mice. In COX-2−/− female mice, the difference was not statistically significant ($P > 0.10$).

Discussion

Differences in bone micro-architecture and bone mineral density are found to be tightly associated with sex and age [3,19,28]. Further studies have demonstrated that genetic influences on the quantity and architecture of trabecular and cortical bone are highly site-specific [14,15]. To determine the effect of COX-2 gene deletion on bone mass and bone architecture, we examined the morphology and bone mineral density at three different anatomic sites of femoral bone in wild-type and COX-2−/− male and female mice at 4 months of age. All male bone, regardless of their genotypes, exhibited superior structural indices at all three regions examined, whereas female bone showed significantly higher bone mineral density at epiphyseal, metaphyseal and cortical bone regions, indicating that the males have a larger volume of better structured bone with a lower mineral content, while the females have a smaller volume of less well structured bone with higher mineralized content. The net effect is nearly identical stiffness between males and females but different material properties (e.g. modulus) which are normalized for the amount and structure of the bone as well as different failure properties (e.g. PYD and ultimate stress) [35]. When comparisons were made between wild-type and COX-2 knockout mice, male mice showed significantly reduced metaphyseal BVF and a significant reduction in bone mineral density at all three regions examined. The reduced bone mineral density in COX-2−/− male was associated with a significantly increased postyield deflection (PYD) in biomechanical testing. Compared to male mice, the deletion of COX-2 had no effect on bone architecture in female mice of the same age but resulted in a trend of decreased bone mineral density within the femoral metaphysis. Taken together, our data suggest that COX-2 is involved in regulation of bone mineral density in mice and the effects resulting from COX-2 deletion are site and sex specific.

A critical role of COX-2 in postnatal high bone turnover such as inflammation or injury has been well established. However, the role of COX-2 on bone morphology and density in the absence of injury or inflammation remains to be elucidated. Previous reports have shown a trend of reduced bone mass, altered architecture and inferior mechanical properties in COX-2−/− mice [1,4]. However, these studies did not take the age and sex into consideration and when normalized by body weight, the differences observed between wild-type and COX-2−/−mice were no longer significant. A recent study by Xu et al. used F1 offspring from the C57/BL6 COX-2+/− and 129/P3J COX-2+/− breeders and demonstrated that there was a decrease in cortical bone width in COX-2−/− male mice at 4 months of age with no differences in bone volume fraction (BVF) in the distal femur. However, by 10 months of age, male mice showed a significantly reduction of BVF in the distal femur, whereas females of the same age group exhibited no significant differences [41]. This result is consistent with our current observation demonstrating sex-dependent alteration of bone morphology in COX-2−/− mice. Since we

utilized the COX-2 breeders that were intercrossed within 129 strain for over 30 generations, it is possible that some difference in bone morphology occurred earlier in their life span. Interestingly, we also found a much lower survival rate of COX-2−/− mice in our colony than that was reported by Xu et al. No significant difference in body weight was found between COX-2−/− mice and wild-type littermates in our colony.

The negative effects of COX-2 gene deletion on bone mineral density suggest a potential side effect that may be associated with persistent inhibition of COX-2. Although the effects of long-term use of COX-2 inhibitors on human bone mineral density and bone remodeling are currently unknown, a few studies find that regular use of non-selective aspirin or NSAIDs may increase BMD in postmenopausal women [2,21,25]. A very recent study which involved multi-centered randomly selected population-based cohorts of 1934 male and 4556 postmenopausal female subjects showed that daily use of COX-2 inhibitor (Celebrex or Vioox) had a sex-specific effect on bone mineral density in human. In older men, daily use of the COX-2 inhibitors was associated with a lower BMD at all hip sites, whereas in postmenopausal woman daily use of COX-2 inhibitors led to a higher bone mineral density than female non-users at most sites examined [32].

The sex-related changes in COX-2−/− mice suggest a link of COX-2 to sex steroid-dependent regulation of bone micro-architecture and bone mineral density. It has been reported that COX-2 expression is induced by 2-fold in bone marrow supernatant harvested from ovariectomized mice; however, it is not clear whether COX-2 induction is associated with bone loss following estrogen deficiency [16]. In addition to estrogen, the role of androgen in regulating bone mineral density and bone structure has also been well established. In combination with mechanical loading, both sex hormones exert larger effects on skeletal structure and bone mineral density than either condition alone. A role of COX-2 in modulating postnatal bone metabolism could be site, age- and sex-dependent, and further studies will be aimed at elucidating interrelations of COX-2 and its metabolites with sex steroids that modulate postnatal bone metabolism.

Acknowledgements

This research is supported by The National Institute of Health AR051469, AR051336, AR46545 and National Science Foundation grants BES-0101239 and EEC-9731643.

References

1. Alam I, Warden SJ, Robling AG, Turner CH. Mechanotransduction in bone does not require a functional cyclooxygenase-2 (COX-2) gene. J Bone Miner Res 2005;20:438–46. [PubMed: 15746988]
2. Bauer DC, Orwoll ES, Fox KM, Vogt TM, Lane NE, Hochberg MC, et al. Aspirin and NSAID use in older women: effect on bone mineral density and fracture risk. Study of Osteoporotic Fractures Research Group. J Bone Miner Res 1996;11:29–35. [PubMed: 8770694]
3. Brodt MD, Ellis CB, Silva MJ. Growing C57Bl/6 mice increase whole bone mechanical properties by increasing geometric and material properties. J Bone Miner Res 1999;14:2159–66. [PubMed: 10620076]
4. Chen Q, Rho JY, Fan Z, Laulederkind SJ, Raghow R. Congenital lack of COX-2 affects mechanical and geometric properties of bone in mice. Calcif Tissue Int 2003;73:387–92. [PubMed: 12874706]
5. Chikazu D, Li X, Kawaguchi H, Sakuma Y, Voznesensky OS, Adams DJ, et al. Bone morphogenetic protein 2 induces cyclo-oxygenase 2 in osteoblasts via a Cbfal binding site: role in effects of bone morphogenetic protein 2 in vitro and in vivo. J Bone Miner Res 2002;17:1430–40. [PubMed: 12162497]
6. Duncan RL, Turner CH. Mechanotransduction and the functional response of bone to mechanical strain. Calcif Tissue Int 1995;57:344–58. [PubMed: 8564797]

7. Forwood MR. Inducible cyclo-oxygenase (COX-2) mediates the induction of bone formation by mechanical loading in vivo. J Bone Miner Res 1996;11:1688–93. [PubMed: 8915776]
8. Goodman S, Ma T, Trindade M, Ikenoue T, Matsuura I, Wong N, et al. COX-2 selective NSAID decreases bone ingrowth in vivo. J Orthop Res 2002;20:1164–9. [PubMed: 12472224]
9. Herschman HR. Prostaglandin synthase 2. Biochem Biophys Acta 1996;1229:125–40. [PubMed: 8555245]
10. Hildebrand T, Laib A, Muller R, Dequeker J, Ruegsegger P. Direct three-dimensional morphometric analysis of human cancellous bone: microstructural data from spine, femur, iliac crest, and calcaneus. J Bone Miner Res 1999;14:1167–74. [PubMed: 10404017]
11. Hildebrand T, Ruegsegger P. Quantification of bone microarchitecture with the structure model index. Comput Methods Biomech Biomed Engin 1997;1:15–23. [PubMed: 11264794]
12. Jee WS, Ke HZ, Li XJ. Long-term anabolic effects of prostaglandin-E2 on tibial diaphyseal bone in male rats. Bone Miner 1991;15:33–55. [PubMed: 1747567]
13. Jiang JX, Cheng B. Mechanical stimulation of gap junctions in bone osteocytes is mediated by prostaglandin E2. Cell Commun Adhes 2001;8:283–8. [PubMed: 12064603]
14. Judex S, Garman R, Squire M, Busa B, Donahue LR, Rubin C. Genetically linked site-specificity of disuse osteoporosis. J Bone Miner Res 2004;19:607–13. [PubMed: 15005848]
15. Judex S, Garman R, Squire M, Donahue LR, Rubin C. Genetically based influences on the site-specific regulation of trabecular and cortical bone morphology. J Bone Miner Res 2004;19:600–6. [PubMed: 15005847]
16. Kawaguchi H, Pilbeam CC, Vargas SJ, Morse EE, Lorenzo JA, Raisz LG. Ovariectomy enhances and estrogen replacement inhibits the activity of bone marrow factors that stimulate prostaglandin production in cultured mouse calvariae. J Clin Invest 1995;96:539–48. [PubMed: 7615826]
17. Kawaguchi H, Raisz LG, Voznesensky OS, Alander CB, Hakeda Y, Pilbeam CC. Regulation of the two prostaglandin G/H synthases by parathyroid hormone, interleukin-1, cortisol, and prostaglandin E2 in cultured neonatal mouse calvariae. Endocrinology 1994;135:1157–64. [PubMed: 8070358]
18. Kawata A, Mikuni-Takagaki Y. Mechanotransduction in stretched osteocytes—temporal expression of immediate early and other genes. Biochem Biophys Res Commun 1998;246:404–8. [PubMed: 9610372]
19. Klein RF, Mitchell SR, Phillips TJ, Belknap JK, Orwoll ES. Quantitative trait loci affecting peak bone mineral density in mice. J Bone Miner Res 1998;13:1648–56. [PubMed: 9797472]
20. Kujubu DA, Fletcher BS, Varnum BC, Lim RW, Herschman HR. TIS10, a phorbol ester tumor promoter-inducible mRNA from Swiss 3T3 cells, encodes a novel prostaglandin synthase/cyclooxygenase homologue. J Biol Chem 1991;266:12866–72. [PubMed: 1712772]
21. Lane NE, Bauer DC, Nevitt MC, Pressman AR, Cummings SR. Aspirin and nonsteroidal antiinflammatory drug use in elderly women: effects on a marker of bone resorption. The Study of Osteoporotic Fractures Research Group. J Rheumatol 1997;24:1132–6. [PubMed: 9195522]
22. Langenbach R, Morham SG, Tiano HF, Loftin CD, Ghanayem BI, Chulada PC, et al. Prostaglandin synthase 1 gene disruption in mice reduces arachidonic acid-induced inflammation and indomethacin-induced gastric ulceration. Cell 1995;83:483–92. [PubMed: 8521478]
23. Mikuni-Takagaki Y. Mechanical responses and signal transduction pathways in stretched osteocytes. J Bone Miner Metab 1999;17:57–60. [PubMed: 10084403]
24. Morham SG, Langenbach R, Loftin CD, Tiano HF, Vouloumanos N, Jennette JC, et al. Prostaglandin synthase 2 gene disruption causes severe renal pathology in the mouse. Cell 1995;83:473–82. [PubMed: 8521477]
25. Morton DJ, Barrett-Connor EL, Schneider DL. Nonsteroidal antiinflammatory drugs and bone mineral density in older women: the Rancho Bernardo study. J Bone Miner Res 1998;13:1924–31. [PubMed: 9844111]
26. O'Banion MK, Sadowski HB, Winn V, Young DA. A serum- and glucocorticoid-regulated 4-kilobase mRNA encodes a cyclooxygenase-related protein. J Biol Chem 1991;266:23261–7. [PubMed: 1744122]
27. Okada Y, Lorenzo JA, Freeman AM, Tomita M, Morham SG, Raisz LG, et al. Prostaglandin G/H synthase-2 is required for maximal formation of osteoclast-like cells in culture. J Clin Invest 2000;105:823–32. [PubMed: 10727451]

28. Orwoll ES, Belknap JK, Klein RF. Sex specificity in the genetic determinants of peak bone mass. J Bone Miner Res 2001;16:1962–71. [PubMed: 11697792]
29. Pilbeam C, Rao Y, Voznesensky O, Kawaguchi H, Alander C, Raisz L, et al. Transforming growth factor-beta1 regulation of prostaglandin G/H synthase-2 expression in osteoblastic MC3T3-E1 cells. Endocrinology 1997;138:4672–82. [PubMed: 9348193]
30. Raisz LG. Prostaglandins and bone: physiology and pathophysiology. Osteoarthr Cartil 1999;7:419–21. [PubMed: 10419786]
31. Raisz LG, Alander CB, Fall PM, Simmons HA. Effects of prostaglandin F2 alpha on bone formation and resorption in cultured neonatal mouse calvariae: role of prostaglandin E2 production. Endocrinology 1990;126:1076–9. [PubMed: 2298153]
32. Richards JB, Joseph L, Goltzman D. The effects of cyclooxygenase-2 inhibitors on bone mineral density: results from the CaMos study. J Bone Miner Res 2005;20:S20.
33. Simon AM, Manigrasso MB, O'Connor JP. Cyclo-oxygenase 2 function is essential for bone fracture healing. J Bone Miner Res 2002;17:963–76. [PubMed: 12054171]
34. Sirois J, Simmons DL, Richards JS. Hormona regulation of messenger ribonucleic acid encoding a novel isoform of prostaglandin endoperoxide H synthase in rat prevulatory follicles. Induction in vivo and in vitro. J Biol Chem 1992;267:11586–92. [PubMed: 1597485]
35. Somerville JM, Aspden RM, Armour KE, Armour KJDMR. Growth of C57BL/6 mice and the material and mechanical properties of cortical bone from the tibia. Calcif Tissue Int 2004;74:469–75. [PubMed: 14961209]
36. Tetradis S, Pilbeam CC, Liu Y, Kream BE. Parathyroid hormone induces prostaglandin G/H synthase-2 expression by a cyclic adenosine 3′,5′-monophosphate-mediated pathway in the murine osteoblastic cell line MC3T3-E1. Endocrinology 1996;137:5435–40. [PubMed: 8940368]
37. Wadhwa S, Choudhary S, Voznesensky M, Epstein M, Raisz L, Pilbeam C. Fluid flow induces COX-2 expression in MC3T3-E1 osteoblasts via a PKA signaling pathway. Biochem Biophys Res Commun 2002;297:46–51. [PubMed: 12220506]
38. Wadhwa S, Godwin SL, Peterson DR, Epstein MA, Raisz LG, Pilbeam CC. Fluid flow induction of cyclo-oxygenase 2 gene expression in osteoblasts is dependent on an extracellular signal-regulated kinase signaling pathway. J Bone Miner Res 2002;17:266–74. [PubMed: 11811557]
39. Wadleigh DJ, Herschman HR. Transcriptional regulation of the cyclooxygenase-2 gene by diverse ligands in murine osteoblasts. Biochem Biophys Res Commun 1999;264:865–70. [PubMed: 10544022]
40. Weinreb M, Machwate M, Shir N, Abramovitz M, Rodan GA, Harada S. Expression of the prostaglandin E(2) (PGE(2)) receptor subtype EP(4) and its regulation by PGE(2) in osteoblastic cell lines and adult rat bone tissue. Bone 2001;28:275–81. [PubMed: 11248657]
41. Xu M, Choudhary S, Goltzman D, Ledgard F, Adams D, Gronowicz G, et al. Do cyclooxygenase-2 knockout mice have primary hyperparathyroidism? Endocrinology 2005;146:1843–53. [PubMed: 15625247]
42. Zhang X, Morham SG, Langenbach R, Young DA, Xing L, Boyce B, et al. Evidence for a direct role of cyclo-oxygenase 2 in implant wear debris-induced osteolysis. J Bone Miner Res 2001;16:660–70. [PubMed: 11315993]
43. Zhang X, Schwarz EM, Young DA, Puzas JE, Rosier RN, O'Keefe RJ. Cyclooxygenase-2 regulates mesenchymal cell differentiation into the osteoblast lineage and is critically involved in bone repair. J Clin Invest 2002;109:1405–15. [PubMed: 12045254]

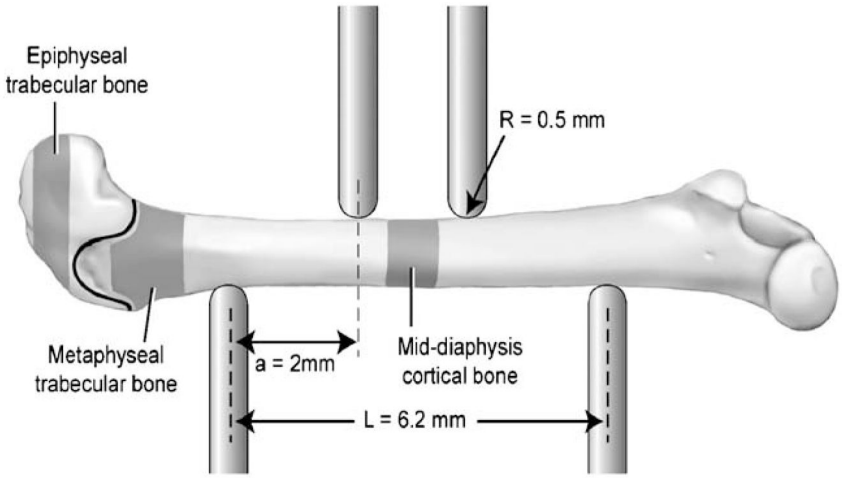

Fig. 1.

Schematic view of 4 point bending setup and typical femur placement. The three volumes of interest scanned in the micro-CT and used for analysis are highlighted, and the growth plate is shown as a black line between the two-trabecular regions. The distance between the two upper points is 2.2 mm (not shown).

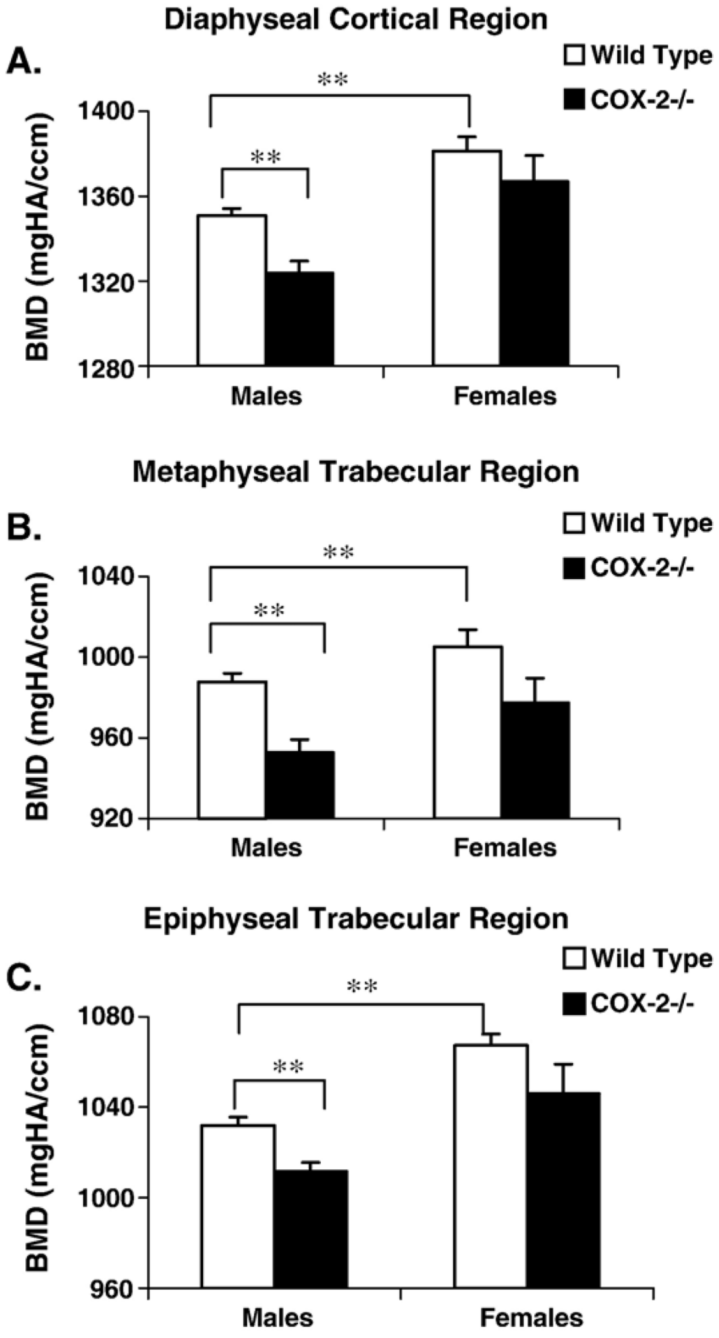

Fig. 2.

Bone mineral densities for male and female mice in the cortial, metaphyseal and epiphyseal regions. Samples were scanned by micro-CT and the values were converted into mineral densities following calibration with hydroxyapatite (HA) phantoms of known densities (mg HA/cm^3). Data shown represent mean ± SEM. ** indicates significance ($P < 0.01$).

Table 1

Femoral cortical bone morphology and geometry in 4-month wild-type and COX-2−/− mice

	Wild type		COX-2	
	Females	**Males**	**Females**	**Males**
Cort. BV. (mm^3)	0.854 (0.022)[a]	1.157 (0.016)	0.873 (0.024)[a]	1.157 (0.035)
Cort.thickness(mm)	0.216 (0.001)[a]	0.242 (0.003)	0.214 (0.002)[a]	0.234 (0.004)
Ant-Pos diameter (mm)	1.32 (0.03)[a]	1.52 (0.02)	1.31 (0.04)[a]	1.56 (0.03)
Med-Lat diameter (mm)	1.62 (0.04)[a]	1.98 (0.02)	1.63 (0.02)[a]	1.96 (0.02)
Avg length (mm)	15.91 (0.09)[a]	16.41 (0.09)	15.88 (0.13)[a]	16.22 (0.08)
I_{ML} (mm^4)	0.127 (0.009)[a]	0.234 (0.01)	0.13 (0.012)[a]	0.243 (0.013)
I_{AP} (mm^4)	0.193 (0.014)[a]	0.384 (0.011)	0.197 (0.012)[a]	0.380 (0.018)

Data are presented as mean (SEM).

[a] Significance between sex ($P < 0.01$).

Table 2

Femoral micro-architecture in 4-month wild-type and COX-2−/− mice

	Wild type		COX-2−/−	
	Female	**Males**	**Females**	**Males**
Metaphyseal region				
BVF	0.1236 (0.0052)[a]	0.3060 (0.0179)[b]	0.1265 (0.0114)[a]	0.258 (0.0269)
Tb.N.	4.4281 (0.1966)[a]	5.9363 (0.1642)	4.4331 (0.2524)[a]	5.786 (0.1540)
Tb.Th	0.0587 (0.0015)[a]	0.0751 (0.0025)	0.0594 (0.0026)[a]	0.0667 (0.0043)
Tb.Sp.	0.2285 (0.0129)[a]	0.1600 (0.0060)	0.2313 (0.0116)[a]	0.1671 (0.0058)
Conn.	43.422 (2.254)[a]	148.45 (8.00)	49.103 (10.988)[a]	122.57 (11.300)
Epiphyseal region				
BVF	0.284 (0.005)[a]	0.417 (0.017)	0.299 (0.016)[a]	0.412 (0.019)
Tb.N.	11.472 (0.266)[a]	11.34 (0.15)	11.718 (0.184)	11.258 (0.107)
Tb.Th	0.063 (0.001)[a]	0.070 (0.002)	0.061 (0.002)[a]	0.067 (0.002)
Tb.Sp	0.113 (0.001)[a]	0.106 (0.002)	0.111 (0.003)[a]	0.104 (0.002)
Conn.	105.322 (7.432)[a]	144.64 (4.622)[b]	139.118 (10.505)[a]	173.730 (6.800)

Data are presented as mean (SEM).

[a] Significance between sex ($P < 0.01$).

[b] Significance between male wild type and COX-2−/− ($P < 0.05$).

Table 3

Femoral mechanical properties in 4-month wild-type and COX-2−/− mice

	Wild type		COX-2	
	Females	**Males**	**Females**	**Males**
Stiffness (N/mm)	242 (14)	247 (14)	223 (11)	246 (18)
Max force (N)	32.1 (1.7)[a]	39.2 (1.2)	33.7 (1.6)[a]	40.2 (1.5)
Yield force (N)	22.6 (12)[a]	28.0 (0.96)	21.9 (1.6)[a]	26.6 (1.1)
Postyield deflection (mm)	0.130 (0.014)	0.157 (0.016)[b]	0.173 (0.021)	0.248 (0.035)
Work (N mm)	4.98 (0.44)[a]	7.52 (0.68)	6.44 (0.68)[a]	9.91 (1.03)
Ultimate stress (MPa)	167.33 (11.54)[a]	126.43 (4.29)	166.05 (9.97)[a]	129.23 (4.68)
Yield stress (MPa)	116.66 (4.99)[a]	90.71 (3.95)	109.68 (8.10)[a]	85.66 (4.29)
E (Gpa)	6.91 (0.67)[a]	3.71 (0.16)	6.09 (0.66)[a]	3.60 (0.23)

Data are presented as mean (SEM).

[a] Significance between sex ($P < 0.05$).

[b] Significance between male wild type and COX-2−/− ($P < 0.05$).